

NASA TECHNICAL NOTE



NASA TN D-3355

c.1

NASA TN D-3355

LOAN COPY: RETURN
AFWL (WLIL-2)
KIRTLAND AFB, NM

0130564



APPLICATION OF ELECTRON PARAMAGNETIC RESONANCE SPECTROSCOPY TO THE STUDY OF SURFACE DEFECTS AND ADSORBED MOLECULES

by Jack H. Lunsford and John P. Jayne

Lewis Research Center

Cleveland, Ohio





APPLICATION OF ELECTRON PARAMAGNETIC RESONANCE
SPECTROSCOPY TO THE STUDY OF SURFACE
DEFECTS AND ADSORBED MOLECULES

By Jack H. Lunsford and John P. Jayne

Lewis Research Center
Cleveland, Ohio

NATIONAL AERONAUTICS AND SPACE ADMINISTRATION

For sale by the Clearinghouse for Federal Scientific and Technical Information
Springfield, Virginia 22151 - Price \$0.30

APPLICATION OF ELECTRON PARAMAGNETIC RESONANCE SPECTROSCOPY TO THE STUDY OF SURFACE DEFECTS AND ADSORBED MOLECULES

by Jack H. Lunsford and John P. Jayne

Lewis Research Center

SUMMARY

A summary of electron paramagnetic resonance theory of free radicals is made and applied to adsorbed gas molecules. The spectra of carbon dioxide and oxygen on magnesium oxide powders are determined. The magnesium oxide was degassed and ultraviolet irradiated prior to the addition of carbon dioxide and oxygen. Ultraviolet irradiation produced a center that is ascribed to an electron trapped in an anion-cation divacancy on the surfaces of the magnesium oxide powder. This center interacts with carbon dioxide and oxygen to form radicals which are thought to be CO_2^- and O_2^- molecule ions. The spectrum of oxygen on zinc oxide was observed and is also attributed to the O_2^- molecule ion. Carbon monoxide gas adsorbs as a paramagnetic species on unirradiated magnesium oxide.

INTRODUCTION

Electron paramagnetic resonance (e. p. r.) spectroscopy is proving to be an extremely useful means for studying surface defects and certain adsorbed species. The requirement that the adsorbed species must have an unpaired electron is not as restrictive as one might think for it now appears that a large number of molecules exhibit paramagnetism upon adsorption. Adsorbed radicals have been detected on metals (ref. 1), semiconductors (ref. 2), and both irradiated and unirradiated insulators (ref. 3). The sensitivity of the technique is quite good with the present limit being about 10^{15} to 10^{16} radicals per gram of adsorbent. This sensitivity, of course, depends on the width of the spectrum. Concentration measurements are more accurate than infrared or visible spectroscopy measurements. Moreover, some very specific information concerning the electronic structure and environment of the species can be gained from the e. p. r. spectrum.

The purpose of this report is to describe how the e. p. r. technique has been used to study three adsorbed species: CO, CO₂⁻, and O₂⁻. The adsorbed CO molecule, as an intermediate species in heterogeneous catalysis, plays an important role in such reactions as the Fisher-Tropsch process. Carbon dioxide represents a class of material that is not particularly electrophilic but apparently adsorbs as a molecular anion provided an accessible electron is present. Oxygen adsorption is particularly interesting because the identification of the adsorbed species has heretofore not been established by the more conventional measurements. The nature of the active sites for adsorption is also discussed since paramagnetic centers on the surface seem to be involved in the formation of CO₂⁻ and O₂⁻. In this work only oxygen adsorption has been studied on zinc oxide whereas the adsorption of oxygen, carbon monoxide, and carbon dioxide was studied on magnesium oxide.

THEORY

In addition to the information that a radical* is formed upon adsorption, two fundamental parameters can be easily determined from the e. p. r. spectra: g values (spectroscopic splitting factors) and hyperfine coupling constants. The g tensor yields more information when the components of the tensor are clearly distinguishable and deviate considerably from the free-spin value of 2.0023. When these conditions are met, the g values reflect the symmetry of the molecule or the defect and elucidate to some degree the energy level configuration. In general, deviations of the g values from 2.0023 are brought about by competing excited states that can combine with the ground state for a given direction of the magnetic field. Those states that involve excitation of the magnetic electron into an outer vacant level give a negative contribution, and those that involve excitation of an inner electron into the half-filled level give a positive contribution to the free-spin g value.

The hyperfine splitting of an e. p. r. line arises from the interaction between the magnetic moment of the unpaired electron and the magnetic moment of nuclei. This interaction may be expressed in a formal way by the spin Hamiltonian (ref. 4).

$$\mathcal{H} = g_e \cdot g_N \cdot \beta \cdot \beta_N \left[\frac{(\bar{L}_e - \bar{S}_e) \cdot \bar{I}_N}{|\bar{r}_e - \bar{r}_N|^3} + \frac{3(\bar{S}_e \cdot \bar{r})(\bar{I}_N \cdot \bar{r})}{|\bar{r}_e - \bar{r}_N|^5} + \frac{8\pi}{3} \cdot \bar{S}_e \cdot \bar{I}_N \cdot \delta(\bar{r}_e - \bar{r}_N) \right] \quad (1)$$

* A free radical is defined here as a molecule, or part of a molecule, in which the normal chemical bonding has been modified so that an unpaired electron is left associated with the system.

where

g_e	g value of electron
g_N	g value of nucleus
β	Bohr magneton
β_N	nuclear magneton
\bar{L}_e	orbital angular momentum operator
\bar{S}_e	electron spin operator
\bar{I}_N	nuclear spin operator
\bar{r}_e	vector position of electron
\bar{r}_N	vector position of nucleus
$\delta(\bar{r}_e - \bar{r}_N)$	Dirac delta function for distance between electron and nucleus, normalized in three dimensions

This Hamiltonian can be divided into two parts. The first,

$$\mathcal{H}^{(1)} = g_e \cdot g_N \cdot \beta \cdot \beta_N \left[\frac{8\pi}{3} \bar{S}_e \cdot \bar{I}_N \cdot \delta(\bar{r}_e - \bar{r}_N) \right] \quad (2)$$

gives the isotropic portion of the hyperfine splitting and is often referred to as the Fermi contact term. The magnitude of this term is a measure of the s-character of a molecular orbital since only s orbitals have a nonzero value for $\delta(\bar{r}_e - \bar{r}_N)$. The magnetic interaction A_{iso} is related to the spin population (a_s^2) of an s orbital by the expression

$$A_{\text{iso}} = g_e \beta \beta_N \frac{8\pi}{3} |\psi_S(0)|^2 a_s^2 \quad (3)$$

Here $\psi_S(0)$ is the amplitude of the wave function of the S orbital at the nucleus. Smith, et al. (ref. 5) have calculated values of A_{iso} for electrons in pure s orbitals associated with carbon-13 nuclei. The ratio of the isotropic portion of the hyperfine splitting, which is experimentally determined, to the A_{iso} term for a pure s orbital, which is termed A_0 , gives the s-state contribution to the molecular orbital.

The remaining part of the Hamiltonian,

$$\mathcal{H}^{(2)} = g_e \cdot g_N \cdot \beta \cdot \beta_N \left[\frac{(\bar{L}_e - \bar{S}_e) \cdot \bar{I}_N}{|\bar{r}_e - \bar{r}_N|^3} + \frac{3(\bar{S}_e \cdot \bar{r})(\bar{I}_N \cdot \bar{r})}{|\bar{r}_e - \bar{r}_N|^5} \right] \quad (4)$$

represents the interaction between two magnetic dipoles, the electron and the nucleus. Such interactions are characteristic of p, d, and higher orbitals. For the molecules studied here, it is reasonable to assume that the interaction arises largely from the p level. The anisotropic hyperfine interactions B_0 have been calculated for pure p orbitals where the hyperfine coupling tensors have cylindrical symmetry (ref. 5). The interaction between the p-state electron and the nucleus can be expressed as a diagonal tensor A , which is axially symmetric. The tensor has the form

$$A = \begin{pmatrix} -\alpha & & \\ & -\alpha & \\ & & 2\alpha \end{pmatrix} \quad (5)$$

Here, 2α is equal to A_{\perp} , the experimentally determined hyperfine coupling constant, when the symmetry axis of the orbital is perpendicular to the external magnetic field. The fraction of p-character that a particular atomic orbital contributes to a molecular orbital is $a_p^2 = 2\alpha/B_0$.

EXPERIMENTAL

Materials

Three types of magnesium oxide have been used, designated MgO I, MgO II, and MgO III. MgO I was prepared from reagent grade powder and contained about 0.001 percent iron (Fe). MgO II and MgO III were prepared from the same reagent grade powder by the addition of $FeCl_3$ to a total of 0.006 and 0.06 percent Fe, respectively. The powders were boiled for several hours in water that contained the $FeCl_3$, extruded into pellets with a hypodermic syringe, and dried in air at $100^{\circ}C$. The boiling step produced a material that consisted of about 95 percent $Mg(OH)_2$. Degassing and decomposition of the hydroxide was carried out by heating the pellets to $800^{\circ}C$ in a vacuum for 16 hours. The formation and decomposition of the hydroxide considerably enhances the surface area of the samples. The B. E. T. surface area that was measured on one sample after this treatment was 170 square meters per gram.

The ZnO samples were prepared from reagent powder, from very high purity material (S. P. 500) that is supplied by the New Jersey Zinc Company, and by thermally decomposing zinc carbonate. After being slurried with water, the zinc oxide paste was extruded into pellets and dried in air at $100^{\circ}C$. The samples used to obtain most of the data were calcined in oxygen at $600^{\circ}C$ for 16 hours and degassed in a vacuum at $400^{\circ}C$ for 2 hours. A few samples were degassed at 500° or $550^{\circ}C$.

The CO_2 (99.99 percent minimum purity), the O_2 (99.6 percent minimum purity) were obtained from a commercial source. These gases were used without further treatment. For one experiment CO was prepared by reducing CO_2 with zinc. The CO_2 was

first frozen at -196°C and the O_2 or other residual gases were removed by evacuation; then the gas was heated for several hours at 550°C in the presence of a zinc film. Mixtures of 57 percent C^{13}O_2 -43 percent C^{12}O_2 and 53 percent C^{13}O -47 percent C^{12}O were also acquired commercially. The $\text{C}^{13}\text{O}-\text{C}^{12}\text{O}$ mixture was deoxygenated by contacting it with a zinc film at 400°C , and condensable gases were removed with a cold trap at -196°C . The $\text{C}^{13}\text{O}_2-\text{C}^{12}\text{O}_2$ mixture was purified by freezing and evacuating at -196°C . A sample of $\text{C}^{13}\text{O}-\text{C}^{12}\text{O}$ was also made from the $\text{C}^{13}\text{O}_2-\text{C}^{12}\text{O}_2$ gas by reduction with zinc.

Procedure

MgO samples used for the O_2 and CO_2 adsorption studies were irradiated with ultraviolet light from a low pressure mercury vapor lamp with an intensity of 60 microwatts per square centimeter at 2537 \AA . Samples were irradiated from 16 to 48 hours, usually in a dynamic vacuum at 10^{-6} torr. After irradiation, the e. p. r. spectrum was recorded. MgO samples used for the CO adsorption studies were not irradiated nor were the ZnO samples.

Adsorption measurements were made with the appropriate gas (CO or CO_2 at approximately 100 torr and O_2 at about 10^{-2} torr), and the new e. p. r. spectra were recorded. The amount of gas adsorbed was determined from the pressure change in an isothermal system of known volume. The pressure was measured with a calibrated direct current thermocouple gage.

Electron Paramagnetic Resonance Measurement

Before the e. p. r. measurement the gases were added to the samples at room temperature. The spectra were recorded at room temperature after the addition of CO or CO_2 . When the adsorbed gas was oxygen, the spectra were usually recorded at -190°C ; however, the spectra were also recorded at room temperature for a few cases. A conventional e. p. r. spectrometer, which operated at a cavity resonance frequency of either 9.1 gigacycles per second (X band) or 35 gigacycles per second (K band) was used to obtain the data. The X-band cavity was a TE 102 type, while the K-band cavity was a right circular cylinder resonant in the TE 011 mode. A nuclear magnetic resonance gauss meter was used to monitor the magnetic field. The g values were obtained by comparison with the value for 2, 2-diphenyl-1-picryl hydrazyl ($g = 2.0036$) and with the value for the Cr^{+3} impurity ($g = 1.9797$) in MgO.

The number of spins associated with a particular line was determined by numerically

integrating the derivative spectrum and comparing with a standard. In the case of CO the standard was pitch in KCl. The estimated error is ± 30 percent. For oxygen the standard was a small single crystal of freshly recrystallized $\text{CuSO}_4 \cdot 5\text{H}_2\text{O}$ ($110 \mu\text{g}$ for the MgO data, $13 \mu\text{g}$ for the ZnO data) that was attached to the side of the sample tube with a commercial varnish. In order that the metal oxide line sample could be compared with these standard point samples the vertical sensitivity variation of the cavity was experimentally determined. An estimated error of ± 20 percent in the number of spins per gram of sample was the result of errors in the weight of the standard, the numerical integrations, and the linear packing density of the sample.

RESULTS AND DISCUSSION

S^1 Center

After several hours of ultraviolet irradiation, the MgO sample assumed a violet color, and the e. p. r. spectrum shown in figure 1 was observed. This spectrum of the

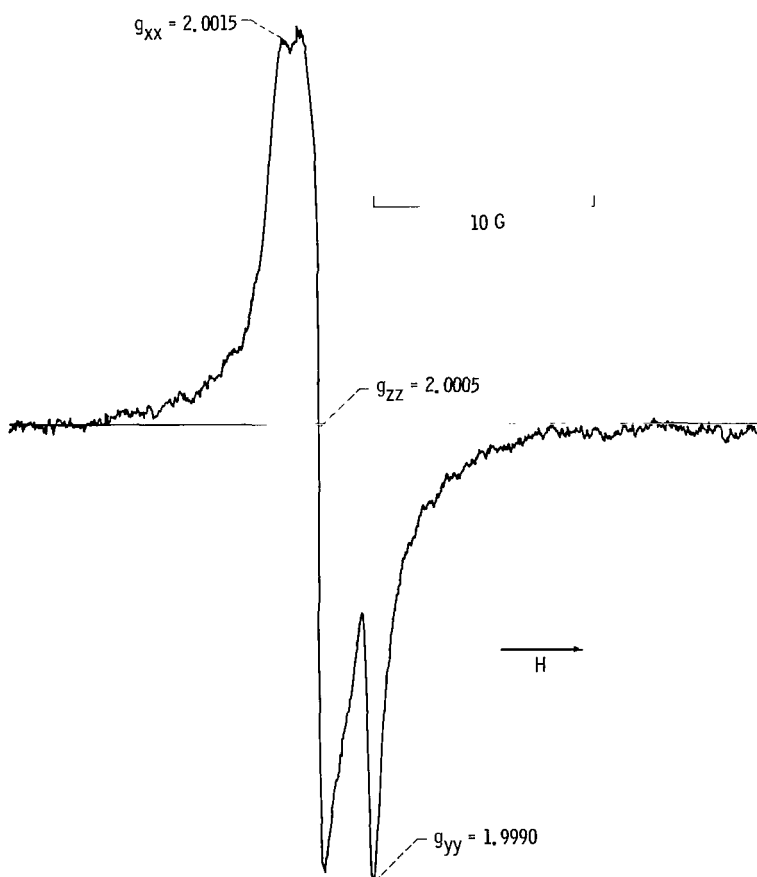


Figure 1. - S^1 spectrum of ultraviolet-irradiated magnesium oxide.

center, which will be designated an S' center, has the g values shown in the figure and listed in table I. The e. p. r. transition can be saturated with a moderate amount of microwave power (approximately 3 mW at room temperature). The paramagnetic species is fairly stable through 100°C , but heating to 200°C for 30 minutes reduces the intensity of the derivative curve by 90 percent. It was further observed that the intensity of the spectrum was greater by a factor of 2 for MgO II than for MgO I.

The formation of surface paramagnetic centers by γ -irradiation of degassed MgO has been reported recently by Nelson and Tench (ref. 6). This type of center, termed an S center, is thought to be an electron trapped at a surface anion vacancy. Ultraviolet light

TABLE I. - TABLE OF g VALUES

Materials	g_{xx}	g_{yy}	g_{zz}
S' center	2.0015	1.9990	2.0005
	± 0.0003	± 0.0003	± 0.0003
S center (ref. 6) ^a	-----	-----	2.0007
	-----	-----	± 0.0002
F_2 center (ref. 7) ^a	-----	-----	2.0008
	-----	-----	± 0.0002
CO ₂ on ultraviolet-irradiated MgO	2.0029	1.9974	2.0017
	± 0.0003	± 0.0003	± 0.0003
CO ₂ ⁻ in γ -irradiated NaCHO ₂ (ref. 10)	2.0032	1.9975	2.0014
	± 0.0002	± 0.0002	± 0.0002
Oxygen on ultraviolet-irradiated MgO	2.077	2.0011	2.0073
	± 0.001	± 0.0003	± 0.0003
Oxygen on ZnO	2.051	2.0020	2.0082
	± 0.001	± 0.0003	± 0.0003
O ₂ ⁻ in NaO ₂ (ref. 15)	2.175	2.000	2.000
	± 0.005	± 0.005	± 0.005
O ₂ ⁻ in KCl (ref. 16)	1.9551	2.4359	1.9512
CO on MgO X-band	2.0055	2.0055	2.0021
	± 0.0003	± 0.0003	± 0.0003
CO on MgO K-band	2.0053	2.0053	2.0018
	± 0.0003	± 0.0003	± 0.0003

^aOnly one apparent g value was reported for these centers since anisotropy is of same magnitude as line width.

with an energy of 4.9 electron volts apparently promotes electrons into traps that exist on the surface of the degassed MgO. The resulting e. p. r. spectrum, shown in figure 1, is characteristic of a center having rhombic symmetry. The similarity in the g value of the S' center to the g value of the S center and the annealing behavior of the centers indicate that they are related; that is, both centers are electrons trapped at a surface defect. The S center, however, does not have rhombic symmetry. If the S' center were an electron trapped at an anion-cation vacancy pair existing in the plane of the surface, rhombic symmetry would be satisfied. One symmetry axis would be along the vacancy pair, and the other axis would be perpendicular to the surface. It should be pointed out that a bulk F_2 center (an electron trapped at an anion-cation vacancy pair) reported by Wertz, et al. (ref. 7) has a g value of 2.0008 ± 0.0002 and a fairly long relaxation time. It shall be assumed for this report that the irradiation-induced paramagnetic center on the surface of the MgO is an electron trapped at an anion-cation vacancy pair in the plane of the surface. The concentration of the cation vacancies is undoubtedly enhanced by the trivalent iron ion through charge compensation (refs. 8 and 9), but the mechanism by which the anion vacancies are formed is not presently known.

CO₂ on Irradiated MgO

Upon exposure to CO₂ or O₂, both the S' center spectrum and the violet color disappear, and new spectra appear. The derivative spectrum for CO₂, recorded at room temperature, is shown in figure 2. The g values of this new spectrum are also listed in table I. Adsorption of CO₂ enriched to 57 percent C¹³ results in two rather broad hyperfine lines symmetrically disposed on each side of the C¹²O₂⁻ spectrum. The amplitude of the hyperfine lines is less than one-tenth of the amplitude of the central line, which is associated with the 47 percent C¹²O₂. Values for the hyperfine coupling constants are listed in table II.

A comparison of the g values for the spectrum of CO₂ adsorbed on ultraviolet irradiated MgO with the spectrum of CO₂⁻ radical ions in γ -irradiated sodium formate (NaCHO₂) single crystals (ref. 10) shows that within experimental error there is complete agreement. Also, the hyperfine coupling constants are quite comparable. As a result of the similarity in the spectra and the analysis in reference 10 of the structure of the CO₂⁻ radical ion, it is concluded that CO₂ adsorbs on irradiated MgO as a nonlinear radical ion. The three g values correspond to the following orientations of the magnetic field with respect to the CO₂⁻ radical: (1) for g_{zz} the magnetic field is parallel to the symmetry axis of the ion, (2) for g_{xx} the magnetic field is perpendicular to the symmetry axis and to the CO₂⁻ plane, and (3) for g_{yy} the magnetic field is perpendicular to the symmetry axis and parallel to the CO₂⁻ plane. The three different g values support

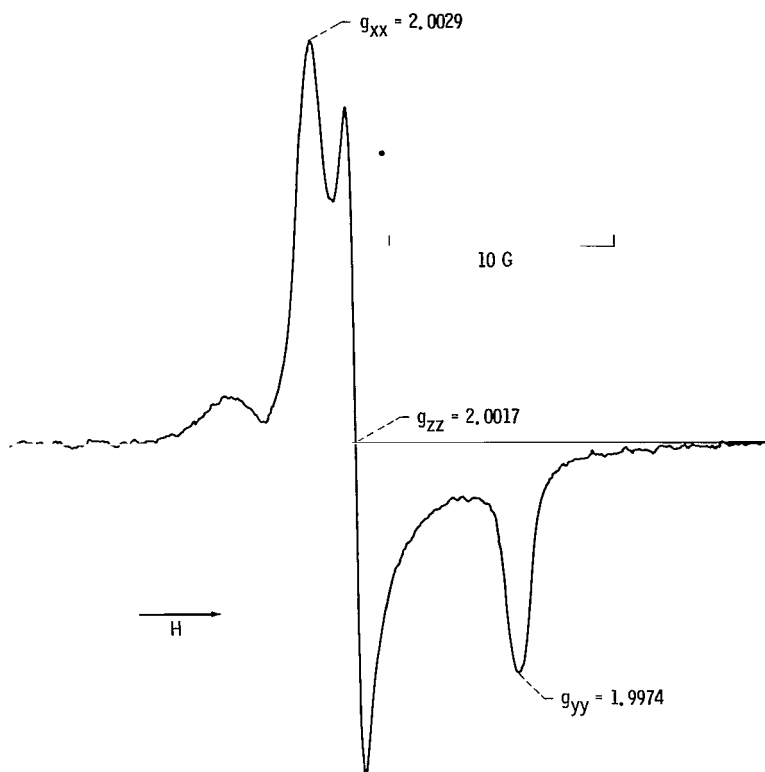


Figure 2. - Electron paramagnetic resonance spectrum of carbon dioxide adsorbed on ultraviolet-irradiated magnesium oxide.

TABLE II. - HYPERFINE VALUES IN GAUSS

Materials	Hyperfine splitting			Hyperfine coupling constants			
	a_{xx}	a_{yy}	a_{zz}	A_{xx}	A_{yy}	A_{zz}	A_{iso}
$C^{13}O_2$ on ultraviolet irradiated MgO	184	184	230	-15	-15	31	199
$C^{13}O_2^-$ in $NaCHO_2$ (ref. 10)	156	151	195	-11	-16	28	167
$C^{13}O$ on MgO	27	11	0	14	-2	-13	13

^aIn powder samples, it was not possible to resolve A_x and A_y .

the concept of a bent structure for the radical ion rather than a linear structure.

The ratio of the s-state contribution of the molecular orbital on the carbon-13 nucleus to a pure 2s orbital on carbon 13 is given by

$$a_s^2 = \frac{A_{iso}}{A_o} = 0.18 \quad (6)$$

The fraction of p-character is

$$a_p^2 = \frac{2\alpha}{B_o} = 0.69 \quad (7)$$

These values may be compared with $a_s^2 = 0.14$ and $a_p^2 = 0.66$ for the CO_2^- radical in NaCHO_2 . If relations given in reference 11 between bond angle and hybridization ratio ρ (where $\rho = a_p/a_s$) are assumed to hold for the adsorbed CO_2 molecule, the OCO bond angle α can be calculated from

$$\alpha = 2 \cos^{-1}(\rho^2 + 2)^{-1/2} \quad (8)$$

With equations (6) to (8), α is calculated to be 131° , which is in agreement with the value of 134° for CO_2^- in NaCHO_2 and for the ONO angle in NO_2 (a molecule isoelectronic with CO_2^-).

The e. p. r. spectrum of carbon dioxide on unirradiated MgO showed no CO_2^- radical ions. Magnesium oxide is a good electrical insulator, which means that there exists a wide forbidden region and that there are no filled electron or hole traps near the conduction or valence bands. The ultraviolet light provides energy for the excitation of electrons to intrinsic defects on the surface where the energy is stored as a trapped electron. Adsorption of a CO_2 molecule by a charge transfer offers then a path to release some of this stored energy.

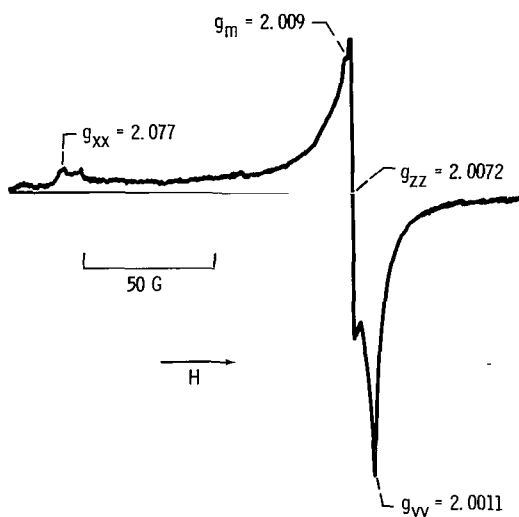


Figure 3. - Derivative spectrum of oxygen adsorbed on ultraviolet-irradiated MgO. Spectrum is recorded at -190°C .

Oxygen on ZnO and MgO

Oxygen on ZnO and MgO were first irradiated with ultraviolet light and then exposed to oxygen. These samples exhibited a new spectrum when cooled to -190°C . This derivative spectrum is displayed in figure 3, and the indicated g values are also listed in table I. The intensity of the spectrum was less for MgO I than for MgO II, in accord with the relative intensities of the S' centers. The number of oxygen molecules adsorbed on the sample equals the number of S' centers. Just part of them, however, formed radicals. Comparison of the results of adsorption measurements with the concentration of S' spins

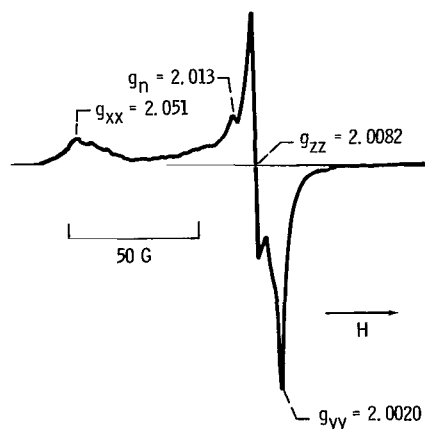


Figure 4. - Derivative spectrum of oxygen adsorbed on degassed ZnO. Spectrum recorded at -190°C .

and oxygen spins showed that the number of oxygen radicals was 40 percent of the number of S' centers.

The spectrum of the radical produced when oxygen was adsorbed on degassed zinc oxide is shown in figure 4. A portion of this spectrum was published earlier by Kokes (ref. 2), but in his paper the low field part was omitted. In agreement with the earlier work (ref. 2) it was found that the number of oxygen spins did not increase linearly with the amount of oxygen adsorbed for residual gas pressures less than 0.5 micron. For higher residual gas pressures the number of oxygen radicals and the number of molecules adsorbed are equal within experimental error. A spectrum comparable to that shown in figure 4 was observed when oxygen was adsorbed on all

of the ZnO samples studied. If the ZnO was degassed at 500°C , however, a slow adsorption process became appreciable; and the oxygen radical spectrum decreased in intensity upon standing at room temperature.

Degassing at elevated temperatures (200° to 250°) after exposure to oxygen showed that the weak lines at $g = 2.009$ and $g = 2.013$ for MgO and ZnO, respectively, are the spectra of a different species, since the weak lines disappear at different temperatures than the main spectra.

The g tensors are the most distinguishing features of the oxygen spectra presented here since there is no hyperfine splitting with the oxygen-16 molecule. It seems clear that the low field portion of the oxygen spectrum for both metal oxides is a part of the whole spectrum. This point is demonstrated when the area above the base line for the derivative spectra is compared with the area below the base line. The two areas should be equal. With the good signal-to-noise ratio that was observed, these areas could be determined accurately and it is apparent that the low field portion of the spectra must be included. Hence, the g tensor has three unique symmetry axes. This can only be true for an atomic radical in orthorhombic or lower symmetry, for a diatomic molecule in an external electric field that has a component perpendicular to the internuclear axis, or for a polyatomic molecule.

The spectrum attributed to the O^- species has been observed in γ -irradiated alkali-metal hydroxide glasses (ref. 12) and x-irradiated calcium fluorophosphate (ref. 13). Each of these materials gives rise to a crystal field of axial symmetry. Qualitatively, the parameters can be explained by postulating a splitting of the $2p$ level such that p_z lies well above p_x and p_y . If this splitting is sufficiently large, g_{zz} should be approximately 2.0023 and $g_{xx} = g_{yy} \gg 2.0023$ (ref. 12). The experimental O^- g values are $g_{zz} = 2.002$, $g_{xx} = g_{yy} = 2.070$ in the hydroxide glasses and $g_{zz} = 2.0012$,

$g_{xx} = g_{yy} = 2.0516$ in the fluorophosphate. An orthorhombic field would also split the p_x and p_y levels; however, it seems improbable that the splitting would be such that $g_{yy} \approx g_{zz} \approx 2.002$, as is the case for the spectra shown in figures 3 and 4.

A similar situation exists for the O_3^- molecule ion. The spectrum of this ion has been observed in γ -irradiated $KClO_3$ (ref. 14) ($g_{zz} = 2.0025$, $g_{xx} = 2.0113$, and $g_{yy} = 2.0174$) and in NaO_3 (ref. 15) ($g_{xx} = g_{yy} = 2.015$, $g_{zz} = 2.003$). Here, too, the splitting is such that $g_{xx} \approx g_{yy} \gg g_{zz}$, which is opposite to the case for the oxygen radical on MgO and ZnO.

Känzig and Cohen have given the following theoretical g values for the O_2^- molecule ion (ref. 16):

$$g_{xx} = g_e + 2 \left(\frac{\lambda^2}{\lambda^2 + \Delta^2} \right)^{1/2} \ell \quad (9)$$

$$g_{yy} = g_e \left(\frac{\Delta^2}{\lambda^2 + \Delta^2} \right)^{1/2} - \frac{\lambda}{E} \left[- \left(\frac{\lambda^2}{\lambda^2 + \Delta^2} \right)^{1/2} - \frac{\Delta^2}{(\lambda^2 + \Delta^2)^{1/2}} + 1 \right] \quad (10)$$

$$g_{zz} = g_e \left(\frac{\Delta^2}{\lambda^2 + \Delta^2} \right)^{1/2} - \frac{\lambda}{E} \left[\left(\frac{\Delta^2}{\lambda^2 + \Delta^2} \right)^{1/2} - \frac{\Delta}{(\lambda^2 + \Delta^2)^{1/2}} - 1 \right] \quad (11)$$

where y is chosen along a $p\pi$ function and x is the internuclear axis. Here λ is an effective spin-orbit splitting of the molecule ion in the field at the surface; Δ and E are defined in figure 5. Further, ℓ represents a correction to the angular momentum about x caused by the surface field; ℓ is unity for the free molecule ion. The free ion would be in a $^2\Pi$ state (ref. 15). If the symmetry about the molecular axis is partially removed, one of the $2p\pi_g$ orbitals will have a higher energy than the other (ref. 15). The expected g values, to first order, will then depend on the ratio of the splitting of these two levels to the spin-orbit coupling coefficient. Zero splitting of the levels would give $g_{xx} = 4$ and $g_{yy} = 0$; and for infinite splitting, with complete orbital quenching, $g_{xx} = g_{yy} = g_{zz} = 2$. The energy levels for an O_2^- molecule ion chemisorbed on a metal oxide surface would be expected to produce some intermediate g values.

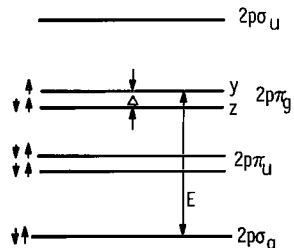


Figure 5. - Occupation of electronic levels of O_2^- in ground state from Känzig and Cohen (ref. 16).

From the experimental g values for the oxygen radical and equations (9) to (11), the parameters λ/Δ , λ/E , and ℓ were calculated. In table III these values are compared with

TABLE III. - VALUES FOR λ/Δ , λ/E , AND ℓ
 CALCULATED FROM EXPERIMENTAL g
 VALUES AND EQUATIONS (9) TO (11)

Materials	λ/Δ	λ/E	ℓ
Oxygen on ultraviolet-irradiated MgO	0.035	0.0032	1.04
O_2^- on ZnO	0.017	0.0032	1.22
O_2^- in KCl (ref. 16)	0.23	0.0025	1.04
O_2^- in NaO_2 (ref. 15)	^a 0.086	-----	-----

^aCalculated after it is assumed that $\ell = 1.04$.

the values for O_2 in KCl (ref. 16) and in NaO_2 (ref. 15). Apparently the low symmetry at the surface of the metal oxides and the strong field gradients cause considerably more splitting of the $2p\pi_g$ levels while only slightly altering the $2p\pi_g - 2p\Delta_g$ splitting. The increased correction to the angular momentum ℓ seems to indicate that the molecule is more restricted on the ZnO than on MgO or in KCl.

The possibility that the oxygen spectra can be attributed to a peroxide group (S-O-O) has been suggested by Kokes (ref. 2). Ingold and Morton have recently reviewed the g values for various oxy and peroxy radicals (ref. 17). It is clear that the g tensors for the oxy and peroxy radicals are neither in agreement with the tensors for the spectra of oxygen on MgO or ZnO nor can they be generated from equations (9) to (11) with one exception. The exception was a radical that was formed in irradiated methanol and ethanol (ref. 17). In addition, there is evidence that the electrons trapped in MgO surface defects are in a metastable state with a rather high potential energy. Moreover, the electron affinity of O_2 is about 1 electron volt (ref. 18). It seems reasonable that the oxygen molecule would form an ionic-type bond upon adsorption, especially since CO_2 , which has a relatively low electron affinity, is able to capture these electrons. The electron, however, may be less localized for the oxygen adsorbed on ZnO.

It is concluded as a result of these considerations that the radical observed on the surface of the metal oxide is O_2^- . The spectra are recorded near liquid nitrogen temperatures because of the short relaxation time of the species at room temperature, and it is not possible to determine from the e. p. r. data alone whether the endothermic reaction



occurs on warming to room temperature. Winter (ref. 18) gives an energy of dissociation of -4.1 electron volt for this reaction, which indicates that the equilibrium would

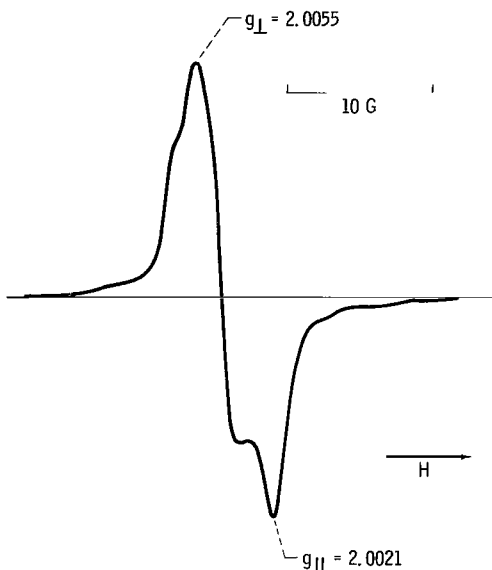


Figure 6. - Electron paramagnetic resonance derivative spectrum of $C^{12}O$ adsorbed on degassed MgO II. Spectrum is recorded at X-band frequencies.

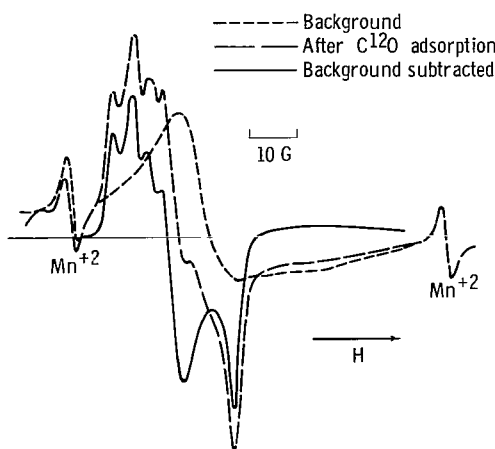
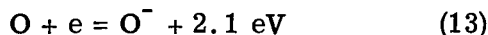


Figure 7. - Electron paramagnetic resonance derivative spectrum of $C^{12}O$ adsorbed on degassed MgO II. Spectrum is recorded at K-band frequencies.

remain shifted far to the left, particularly on MgO where the number of free electrons is limited. On ZnO, where the free electrons become more available on warming, the reaction



must be considered, and the possibility for dissociation of the O_2^- ion is somewhat more favorable.

CO on MgO

Upon exposure of the degassed (but not irradiated) MgO to CO, the X-band spectrum shown in figure 6 was observed. The spectrum grew in intensity for about 20 days. The rate of growth as well as the final intensity of the spectrum increased with the iron content of the sample (though not linearly). After 20 days the intensity of the spectra for MgO I, MgO II, and MgO III was in the ratio 1.0 to 1.6 to 2.0. While the X-band spectrum of the evacuated MgO has no background lines at the magnetic fields of interest, the K-band spectrum showed an interfering line, which is believed to be the spectrum of Fe^{+3} ions (ref. 19). This line appeared at the higher frequencies because the sensitivity of the instrument is more than an order of magnitude greater in this region, and because the polycrystalline Fe^{+3} line is reduced in width while the CO line becomes broader. Since the total number

of spins contributing to the CO and the iron lines is independent of frequency, the amplitude of the lines must correspondingly increase or decrease. In figure 7 the iron spectrum has been subtracted out to give the resulting K-band $C^{12}O$ spectrum. The g values for the X- and K-band spectra are listed in table I (p. 7). The e. p. r. transition begins to saturate at approximately 1 milliwatt of microwave power at room temperature.

With the $C^{13}O-C^{12}O$ mixture on the sample, the spectrum at X-band is shown in figure 8. Of particular interest are the hyperfine lines on each side of the $C^{12}O$ spectrum. In figure 8 the overlapping $C^{12}O$ spectrum is subtracted from the high field side so that

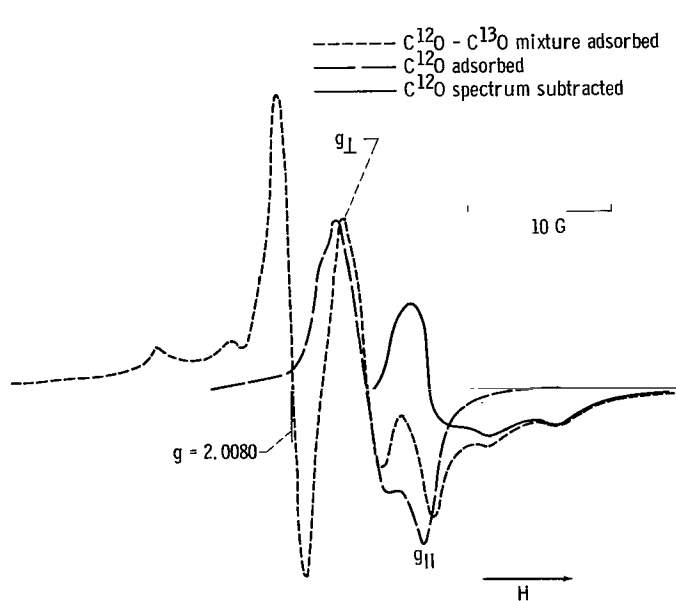


Figure 8. - Electron paramagnetic resonance derivative spectrum of 53 percent $C^{13}O$ -47 percent $C^{12}O$ mixture at X-band frequencies. $C^{12}O$ spectrum is subtracted to display high field hyperfine spectrum.

the $C^{13}O$ spectrum can be clearly displayed. Values for the hyperfine coupling constants are listed in table II (p. 9). The other line with $g=2.0080$ has not been identified. It was at first believed to be an impurity in the $C^{13}O$ - $C^{12}O$ mixture; however, several observations indicate otherwise. The low field line grew at the same rate and was removed at the same rate as the $C^{12}O$ line. Furthermore, the ratio of intensities remained the same whether the starting gas was purified CO or was made from CO_2 . The unknown line was not present in the $C^{12}O$ made from CO_2 , which indicates that any impurities originating during the exposure to zinc did not

produce the line. It should also be pointed out that the line did not appear relatively as strong at K-band frequencies.

Results of desorption studies and spin concentration measurements for CO on MgO show that about 5 percent of the adsorbed CO forms a radical.

The $C^{12}O$ e. p. r. spectra that are shown in figures 6 and 7 are clearly the result of the uniaxial anisotropy of the g tensor (ref. 20). For the $C^{12}O$ spectrum the effect is the result of the anisotropic g tensor rather than the hyperfine splitting since the spectrum observed at two frequencies leads to the same g values. It is interesting to note that the calculated curves of Lebedev show that g_{\perp} is slightly to the high field side of the first major maximum peak when the line width of the individual components is of the same magnitude as the g factor anisotropy (ref. 20). This point has been considered in determining the g_{\perp} values shown in table I (p. 7). The uniaxial anisotropy is certainly consistent with a linear CO molecule. Since g_{\perp} is larger than the free electron g values of 2.0023, it may be concluded that there are excited states which can combine with the ground state of the adsorbed molecule for a given direction of the magnetic field. These involve excitation of an inner electron into the half-filled level that contains the magnetic electron.

The spectrum shown in figure 8 is somewhat more difficult to analyze because of anisotropic g values and anisotropic hyperfine coupling constants; however, the results are believed to be definitive. Theoretical spectra resulting from hyperfine interactions in polycrystalline materials have been reported in the literature (ref. 20). To determine

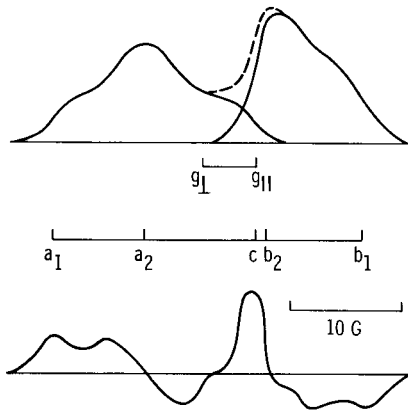


Figure 9. - Theoretical spectrum for $C^{13}O$ with hyperfine interactions shown in figure. Upper curve is absorption spectrum, while lower curve is derivative spectrum. $a_1 b_1 = a_x$; $a_2 b_2 = a_y$; $c c = a_z = 0$.

contribution in the adsorbed $C^{13}O$ molecule to the pure $2s$ orbital on a C^{13} nucleus is given by

$$a_s^2 = \frac{A_{iso}}{A_o} = 0.01 \quad (14)$$

Should the electron be in the p state, the interaction with the nucleus is of the dipole dipole type. This interaction can be expressed as a diagonal tensor A , which is axially symmetric. The tensor has the form

$$A = \begin{pmatrix} -\alpha & & \\ & -\alpha & \\ & & 2\alpha \end{pmatrix} \quad (5)$$

The experimental anisotropic hyperfine interaction tensor A_{exp} is not axially symmetric but may be resolved into two axially symmetric tensors A_1 and A_2 , with the symmetry axis along the x and y axes, respectively. Here,

$$A_{exp} = A_1 + A_2 = \begin{pmatrix} 2\alpha & & \\ & -\alpha & \\ & & -\alpha \end{pmatrix} + \begin{pmatrix} -\beta & & \\ & -\beta & \\ & & 2\beta \end{pmatrix} \quad (15)$$

The $2p_x$ character of the molecular orbital $a_{p_x}^2$ is equal to $2\alpha/B_o$ where B_o is the theoretical value for an electron in a pure p orbital. Likewise, the $2p_y$ character $a_{p_y}^2$ is equal to $2\beta/B_o$. From the hyperfine constants of table II, the tensor may be

resolved into

$$A_{\text{exp}} = \begin{pmatrix} 14 & & \\ & -13 & \\ & & -2 \end{pmatrix} = \begin{pmatrix} 18.0 & & \\ & -9.0 & \\ & & -9.0 \end{pmatrix} + \begin{pmatrix} -3.6 & & \\ & -3.6 & \\ & & 7.3 \end{pmatrix} \quad (16)$$

The values of $a_{p_x}^2$ and $a_{p_y}^2$ are, therefore, equal to 0.28 and 0.11, respectively.

The sum of $a_{p_x}^2$, $a_{p_y}^2$, and a_s^2 gives the fraction of the electron that is associated with the C^{13} nucleus. From this analysis it is apparent that the unpaired electron is about 40 percent on the carbon (ref. 21), and is essentially in a pure p-atomic orbital.

The following molecular orbitals of free carbon monoxide are (ref. 22): (1) three occupied σ orbitals, corresponding to unshared pairs on the carbon and oxygen atom and a σ bond between these atoms, (2) an occupied doubly degenerate π orbital that contains four electrons, (3) an empty strongly antibonding σ orbital, and (4) a strongly antibonding π orbital. In forming a metal carbonyl it is postulated that there is a simultaneous transfer of an electron from the σ orbital of the CO molecule to the metal, and from the metal to an antibonding π orbital (ref. 22). This process would result in an unpaired electron in a pure π orbital, and hence the atomic s-character with respect to the carbon atom should be very small.

The e. p. r. evidence indicates that about 5 percent of the CO molecules are adsorbed in a manner similar to that just described; that is, electrons were transferred from the carbon σ orbital to a surface site, while the same site contributed an electron to the antibonding π orbital of the CO. The concept that CO forms a neutral radical rather than a radical anion is supported by the evidence that CO did not react rapidly with the S' defect electron as did the CO_2 and O_2 molecules.

The adsorption site for the formation of the radical is of interest. Since the radical concentration increased with the iron content, it seems that the iron plays a significant role, either as the adsorption site or in forming surface defects which are adsorption sites. This aspect of the problem is currently being investigated.

CONCLUSIONS

From a study of the e. p. r. spectra of adsorbed gases the following conclusions were drawn:

1. Carbon dioxide adsorbs on ultraviolet-irradiated magnesium oxide by interacting with an electron trapped at a surface defect. The electron becomes localized on the carbon dioxide and the CO_2^- molecule ion is formed.

2. Oxygen adsorbs on zinc oxide and ultraviolet-irradiated magnesium oxide as a radical that is believed to be the O_2^- molecule ion.

3. Approximately 5 percent of the carbon monoxide that adsorbs on magnesium oxide forms a paramagnetic species. The anisotropic g values and hyperfine constants along with the concepts for bonding in metal carbonyls indicate that this radical is a linear molecule with the unpaired electron in a π -antibonding orbital.

Lewis Research Center,
National Aeronautics and Space Administration,
Cleveland, Ohio, July 15, 1965.

REFERENCES

1. Turkevich, J. ; Nozaki, F. ; and Stamires, D. : Studies on Nature of Active Centers and Mechanism of Heterogeneous Catalysis. Proc. Third Int. Cong. on Catalysis, North-Holland Pub. Co. , 1965, pp. 586-595.
2. Kokes, R. J. : The Study of Oxygen Species on Zinc Oxide by Electron Spin Resonance. Proc. Third Int. Cong. on Catalysis, North-Holland Pub. Co. , 1965, pp. 484-492.
3. Kohn, Harold W. : Paramagnetic Studies of Radiation Damage in Silica Gel. J. Chem. Phys. , vol. 33, no. 5, Nov. 1960, p. 1588.
4. Ingram, D. G. E. : Free Radicals as Studied by Electron Spin Resonance. Butterworths Sci. Pub. , London, 1958, p. 103.
5. Smith, W. V. ; Sorokin, P. P. ; Gelles, I. L. ; and Lasher, G. J. : Electron-Spin Resonance of Nitrogen Donors in Diamond. Phys. Rev. , vol. 115, no. 6, Sept. 15, 1959, pp. 1546-1552.
6. Nelson, R. L. ; and Tench, A. J. : Chemisorption and Surface Defects in Irradiated Magnesium Oxide. J. Chem. Phys. , vol. 40, no. 9, May 1, 1964, pp. 2736-2737.
7. Wertz, J. E. ; Orton, J. W. ; and Auzins, P. : Electron Spin Resonance Studies of Radiation Effects in Inorganic Solids. Disc. Faraday Soc. , no. 31, 1961, pp. 140-150.
8. Lunsford, Jack H. : A Study of Irradiation-Induced Active Sites on Magnesium Oxide Using Electron Paramagnetic Resonance. J. Phys. Chem. , vol. 68, no. 8, Aug. 1964, pp. 2312-2316.
9. White, J. : Properties of Non-Stoichiometric Compounds. Trans. Brit. Ceramic Soc. , vol. 56, 1957, pp. 553-568.

10. Ovenall, D. W. ; and Whiffen, D. H. : Electron Spin Resonance and Structure of the CO_2^- Radical Ion. *Mol. Phys.*, vol. 4, no. 2, 1961, pp. 135-144.
11. Atkins, P. W. ; Keen, N. ; and Symons, M. C. R. : Oxides and Oxyions of the Non-metals. II. CO_2^- and NO_2 . *J. Chem. Soc.*, 1962, pp. 2873-2880.
12. Blandamer, M. J. ; Shields, L. ; and Symons, M. C. R. : Unstable Intermediates. Pt. XXIII. Solvated Electrons: Stabilization in Aqueous Alkali-Metal Hydroxide Glasses. *J. Chem. Soc.*, Nov. 1964, pp. 4352-4357.
13. Segall, B. ; Ludwig, G. W. ; Woodbury, H. H. ; and Johnson, P. D. : Electron Spin Resonance of a Center in Calcium Fluorophosphate. *Phys. Rev.*, vol. 128, no. 1, Oct. 1, 1964, pp. 76-79.
14. Atkins, P. W. ; Brivati, J. A. ; Keen, N. ; Symons, M. C. R. ; and Trevalion, P. A. : Oxides and Oxyions of the Nonmetals. Pt. III. Oxy-Radicals of Chlorine. *J. Chem. Soc.*, 1962, pp. 4785-4793.
15. Bennett, J. E. ; Ingram, D. J. E. ; and Schonland, D. : Paramagnetic Resonance Spectra of the Alkali Superoxides and Chlorine Dioxide. *Proc. Phys. Soc.*, ser. A, vol. 69, pt. 7, July 1956, pp. 556-565.
16. Känzig, W. ; and Cohen, M. H. : Paramagnetic Resonance of Oxygen in Alkali Halides. *Phys. Rev. Letters*, vol. 3, no. 11, Dec. 1, 1959, pp. 509-510.
17. Ingold, K. U. ; and Morton, J. R. : Electron Spin Resonance Spectra of Organic Oxy Radicals. *J. Am. Chem. Soc.*, vol. 86, no. 16, Aug. 20, 1964, pp. 3400-3402.
18. Winter, E. R. S. : The Reactivity of Oxide Surfaces. *Advances in Catalysis*. Vol. 10. Academic Press, 1958, pp. 196-241.
19. Lunsford, Jack H. : Polycrystalline EPR Spectrum of Fe^{3+} Ions in MgO. *J. Chem. Phys.*, vol. 42, no. 7, Apr. 1, 1965, pp. 2617-2618.
20. Lebedev, Y. S. : Calculation of Electron Paramagnetic Resonance Spectra with an Electronic Computer. II. Asymmetrical Lines. *J. Structural Chem. (USSR)*, vol. 4, Jan. -Feb. 1963, pp. 19-24.
21. Blyholder, G. : Molecular Orbital View of Chemisorbed Carbon Monoxide. *J. Phys. Chem.*, vol. 68, no. 10, Oct. 1964, pp. 2772-2778.
22. Orgel, L. E. : An Introduction to Transition Metal Chemistry. John Wiley & Sons, Inc., 1960, pp. 135-137.

"The aeronautical and space activities of the United States shall be conducted so as to contribute . . . to the expansion of human knowledge of phenomena in the atmosphere and space. The Administration shall provide for the widest practicable and appropriate dissemination of information concerning its activities and the results thereof."

—NATIONAL AERONAUTICS AND SPACE ACT OF 1958

NASA SCIENTIFIC AND TECHNICAL PUBLICATIONS

TECHNICAL REPORTS: Scientific and technical information considered important, complete, and a lasting contribution to existing knowledge.

TECHNICAL NOTES: Information less broad in scope but nevertheless of importance as a contribution to existing knowledge.

TECHNICAL MEMORANDUMS: Information receiving limited distribution because of preliminary data, security classification, or other reasons.

CONTRACTOR REPORTS: Technical information generated in connection with a NASA contract or grant and released under NASA auspices.

TECHNICAL TRANSLATIONS: Information published in a foreign language considered to merit NASA distribution in English.

TECHNICAL REPRINTS: Information derived from NASA activities and initially published in the form of journal articles.

SPECIAL PUBLICATIONS: Information derived from or of value to NASA activities but not necessarily reporting the results of individual NASA-programmed scientific efforts. Publications include conference proceedings, monographs, data compilations, handbooks, sourcebooks, and special bibliographies.

Details on the availability of these publications may be obtained from:

SCIENTIFIC AND TECHNICAL INFORMATION DIVISION
NATIONAL AERONAUTICS AND SPACE ADMINISTRATION

Washington, D.C. 20546